A new disaggregation induced emission enhancement (DIEE)based probe for cellular detection of copper and lactate

Nidhi Gour[a]*, Vivek Shinh Kshtriya, Deepak Kumar Pandey, Sumit Kharbanda[b], Chandra Kanth P[a], Manoj Pandey, Dheeraj K Singh, Dhiraj Bhatia[b],

[a] Department of Medicinal Chemistry, Indian Institute of Advanced Research, Gandhinagar, Gujarat, 382426, India; E-mail: nidhi.gour@iar.ac.in; gournidhi@gmail.com*Tel: +91 79 30514142: Fax*

{b} Department of Physics, IITRAM, Ahmedabad

[c] Biological Engineering Discipline, Indian Institute of Technology Gandhinagar (IIT Gandhinagar), Palaj, Gandhinagar 382355, Gujarat, India; Ph no: +91-79-2395-2537

[d] Department of Science, School of Technology, Pandit Deendayal Petroleum University, Gandhinagar, Gujarat, India

Abstract: We report self assembling/aggregation properties of acyl-thiourea derivative, N-((6-methoxy-pyridin-2-yl)carbamothioyl)benzamide(**NG1**) and the disaggregation induced emission which leads to its application as fluorescence and colorimetric probe for the sensitive detection of Cu^{2+}. The microscopy analysis of **NG1**via SEM, and AFM reveal that it self-assembles to give fiber-like morphologies.Interestingly,**NG1** also assembles to fluorescent fibers which show tunable emission properties. Addition of $Cu^{2+}$to these fibers causedisruption/disaggregation of fibers and a golden yellow fluorescence is produced due to disaggregation induced emission enhancement (DIEE). The application of **NG1** as selective sensor for copper was further assessed by UV visible and fluorescence spectroscopy. Limit of Detection(LOD) of Cu^{2+} with colorimetry was 2.5ppm while LOD of Cu^{2+} with fluorescence was as low as 0.1ppm. This yellow fluorescence is quenched after the addition of lactic acid and hence **NG1** could potentially be used for the sequential detection of both Cu and lactate.Further, structural modification of the probe **NG1** suggest crucial role of both pyridine and acyl-thiourea moiety in the binding of Cu^{2+}. The experimental results of interaction of **NG1** with Cu^{2+} and lactate were also validated theoretically by quantum chemical calculations based on density functional theory (DFT). Finally, we explore the ability of **NG1**for the sequential detection of Cu^{2+} and lactate in cells, which suggests**NG1** can be used effectively for the cellular imaging applications and to selectively sense Cu^{2+}. To, the best of our knowledge,

this is the first report wherein a dual sensor for $Cu^{2+}$and lactate ion is synthesized and it may in allpossibilities pave the way for the diagnosis of Cu^{2+}associated disorders like Wilson's disease and in the detection of elevated lactate levels which are associated with the wide range of pathologies likemitochondrial diseases, cerebral ischemia and cancer.

Key words: Copperand Lactic acid detection; Disaggregation-induced emission enhancement (DIEE); Self-assembly; Cell imaging; DFT calculations

Introduction

There is ever increasing need to develop new optical probes which could detect analyte with high sensitivity and good signal amplification. Various mechanisms are used to develop novel sensor molecules which includes photo-induced electron transfer (PET),[1]intramolecular charge transfer(ICT)[2], Fluorescence resonance energy transfer,[3]aggregation-induced emission (AIE),[4]processes. Another very important sensing mechanism which can be utilized for the development of sensitive probes can be disaggregation induced emission enhancement (DIEE).[5]DIEE probes have very low fluorescence or are non-fluorescent in aggregated state and the fluorescence is enhanced ondisaggregation.[6]Disaggregation of the aggregated probe leads to remarkable enhancement of emission and signal amplification. There are few literature reports which cite ''disaggregation'' as the mechanism for fluorescence enhancement, however such reports are very limited and not many research groups have explored this phenomenon.[7-9] Even, the aggregation behavior of probe is seldom discussed and there are very few reports which show self-assembling properties and microscopy analysis of probe. Due to this the concept, of DIEE is poorly understood and even if the probe is exhibiting sensing property due to DIEE the researchers remain unaware of it.[10] Althoughvery limited literature have already been reported utilizing this mechanism to develop novel probes, the role of ''disaggregation'' in probe development is not much explored. As a result of the poorly established concept, a proper interpretation of the data or an active application of disaggregation for novel probe design has been hampered. As a result even if the "disaggregation" may be the real underlying mechanism, researchers remain unaware about it due to lack of microscopy analysis.Hence the self-assembly/aggregation properties of the probe should be adequately discussedwhile deciphering the mechanism of sensing.

Herein, we have reported self-assembling/aggregation behavior of a new probeN-((6-

methoxypyridin-2-yl)carbamothioyl)benzamide(NG1) to fibers extensively via microscopy analysis. These self-assemblies get disaggregated on addition of Cu^{2+} and the disaggregation of the aggregated probe results in the golden yellow fluorescence which could be visualized by naked eye. This phenomenon is extensively studied by microscopy techniques like SEM, AFM and Fluorescence microscopy. The DIEE caused by the addition of Cu^{2+} ions to **NG1** has been used to design a sensor for the selective and sensitive detection of Cu^{2+}.Cu^{2+} is an essential micronutrient,howeverif the concentration of Cu^{2+} increases beyond a threshold, it causes deleterious effects on kidney, liver and gastrointestinal tracts and lead to diseases like Alzheimer's,[11] Parkinson's[12] and Wilson's disease.[13] Hence developing a selective and sensitive probe which could detect copper at very minute level is of significant importance. It was further noted that addition of lactic acid causes quenching of fluorescence of **NG1**-Cu^{2+} complex hence, the novel probe can also be used for sequential detection of Cu^{2+} as well as lactate. Lactic acid like Cu^{2+} is also very harmful at concentrations above threshold and many diseases like mitochondrial diseases, cerebral ischemia and cancer are associated with high lactate levels in blood.[14]Combined experimental tools (UV-visible, fluorescence, FTIR and NMR spectroscopy) and quantum chemical calculations based on density functional theory (DFT) were used for the sequential identification of Copper II (Cu^{2+}) and lactic acid by florescent probe NG1.[15]

3. Results and discussion

The chemical synthesis of **NG1** was carried out in ……..step by the scheme shown in figure below….. Once the chemical structure of **NG1**was characterized thoroughly by NMR and mass spectroscopy and its purity was ascertained and we studied the self-assembling properties of the NG1**.** For self-assembly studies **NG1** was dissolved at 1mM concentration in 70% methanol water**.** The Scanning electron microscopy (SEM)image of **NG1** reveals it assembled to fiber like morphologies. The diameter of these fibers were 200-400 nm and the length varied to several micrometer range. The AFM micrograph studies further reveal that the fiber morphology changes as the solvent polarity and the concentration of NG1 is changed.

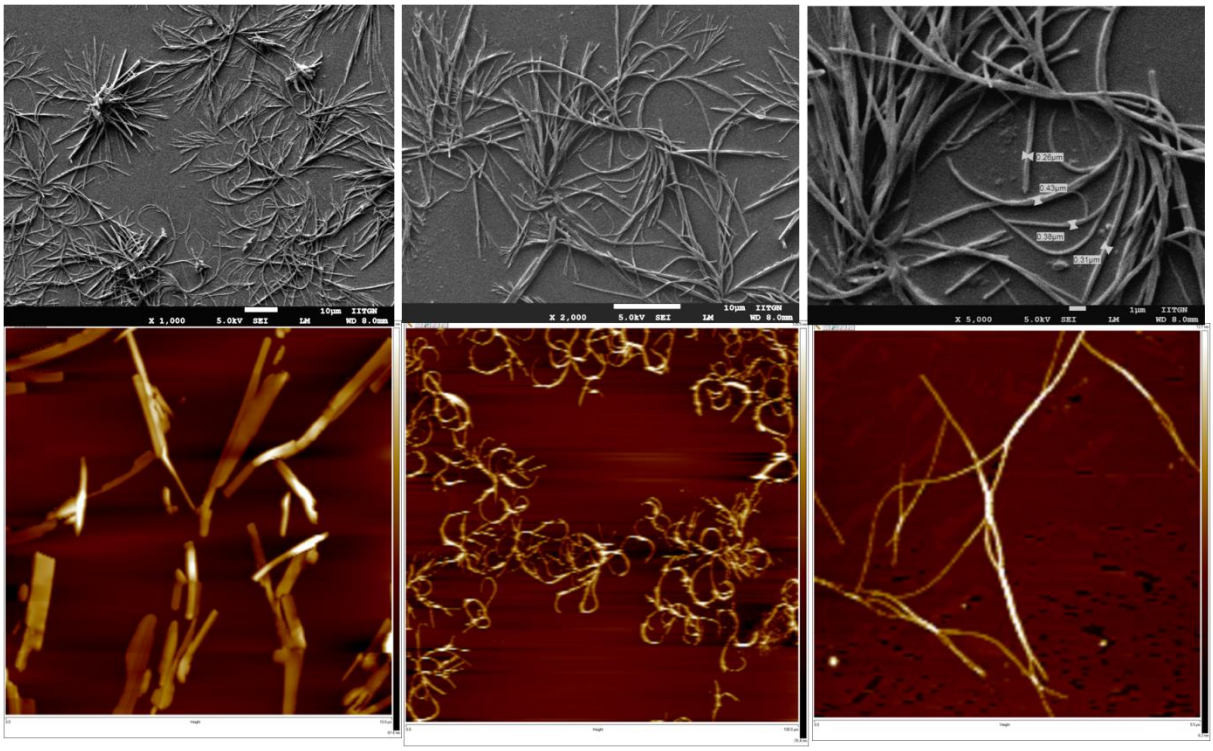

Figure 1: Fibers formed by self-assembly of **NG1**. SEM image of **NG1** at (a) 10 μm (b) 2 μmscale (c) 1-micron scale image showing diameter of fiber of NG1 formed by self-assembly of NG1; AFM images of NG1 (d) Methanol alone; (e) 70% methanol: water showing coiling of fibers which could be also seen in SEM (f) Twisting of fibers on dilution of(e).

The fibers formed by the self-assembly of **NG1**were also studied extensively via optical and fluorescence microscopy. It was noted that **NG1** fibers exhibits fluorescence and appeared blue, green and red under blue, green and red filter. The fibers exhibitpanchromatic fluorescence and tunable emission with different excitation wavelengths. The emission spectra of **NG1** also changed in accordance to the excitation wavelength (Fig. ESI). It may be surmised that **NG1** assembled to aggregates which show tunable emission albeit with low fluorescence intensity.

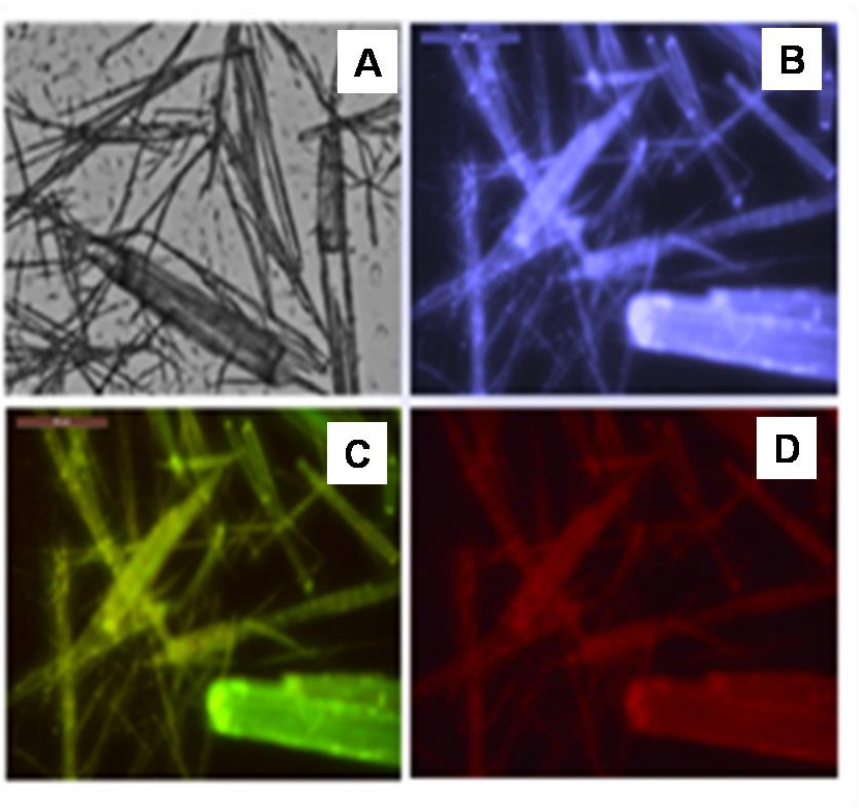

Figure 2: Self-assembly of NG1 to fibers having tunable emission properties (a) Bright field; (b) Blue filter (c) Green filter (d) Red filter.

Interestingly, when Cu^{2+} was added to these fibers, disruption of febrile assembly occurs. It is also evident that the colorless solution of**NG1** turned to golden yellow on addition of Cu^{2+}. The fluorescence produced was very intriguing to us and we decided to first assess whether this fluorescence is produced only by Cu^{2+} or other metal ion as well. Notably, we found that the yellow fluorescence is produced only on addition of Cu^{2+} and not with any other ion (Fig.). Hence, we decided to study the utility of **NG1** for detection of Cu^{2+} extensively via UV visible and Fluorescence spectroscopy.

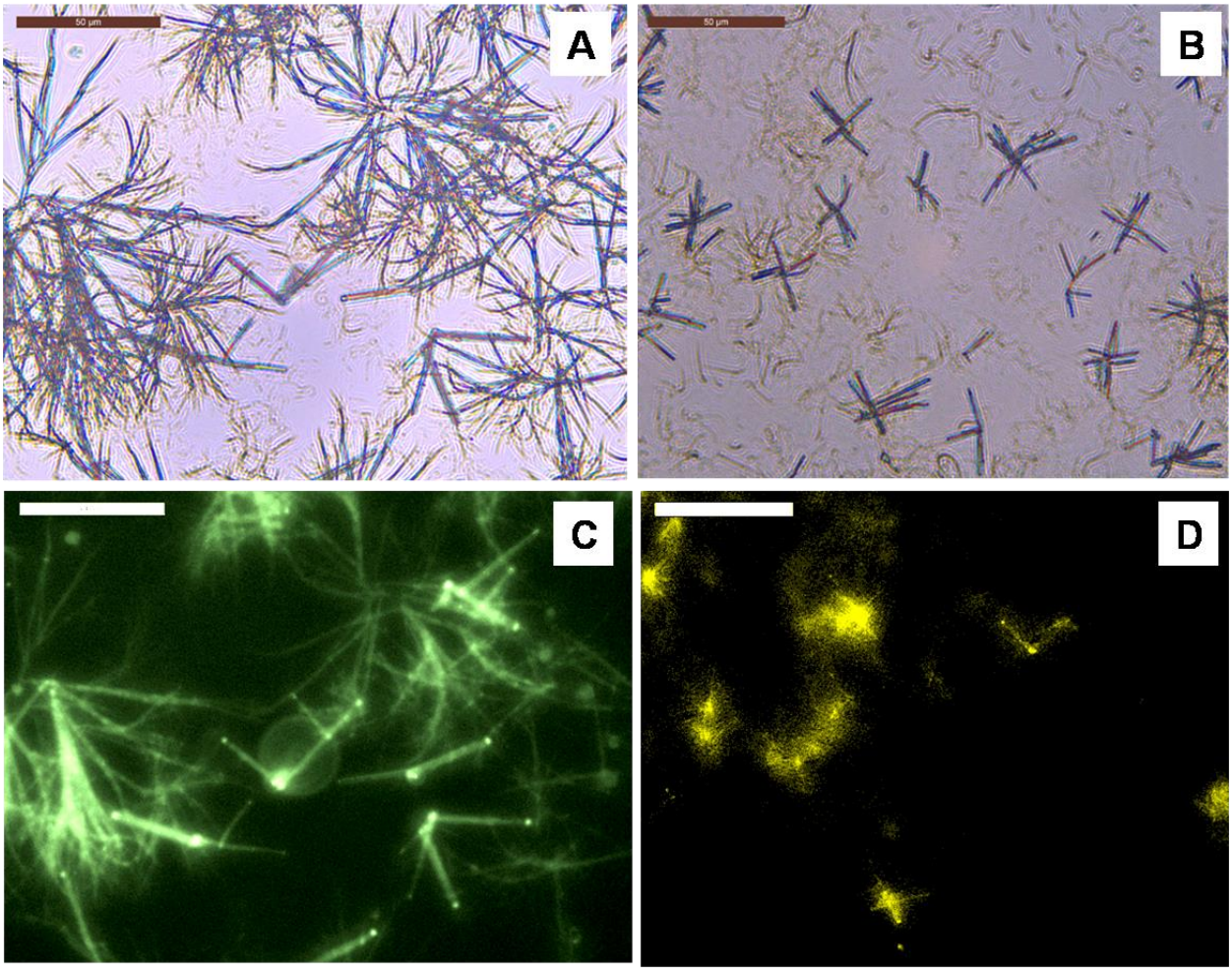

Figure 3: Disaggregation of fibers in the presence of Cu^{2+} (a) Bright field image of **NG1;**(b) Bright field image of **NG1**withCu^{2+};(c) Fibers exhibits green fluorescence under green filter; (d) Disruption of fibers in presence of $Cu^{2+}$and yellow fluorescence could be seen.

The yellow color produced by the disaggregation of fibers of **NG1** on addition of Cu^{2+} indicated that **NG1** forms complex with Cu^{2+} and it could potentially be used for detection of Cu^{2+}. Hence to study the interaction of**NG1**with Cu^{2+}in more detail,the absorption spectra of probe **NG**1 was studied in the presence of different ppm of Cu^{2+} by UV−visible spectroscopy. As shown in Fig. 2A **NG1**exhibited a maximum absorption at ~287 nm. On gradual addition of Cu^{2+}, the absorption intensity at ~287 nm decreases whereas an additional absorption appears simultaneously at ~340 nm through an isosbestic point at 320 nm. The intensity of this peak increases as the concentration of Cu^{2+} (0-50 ppm) increases and is ascertained to the formation of

aggregated complex state **NG1**-Cu^{2+} (Fig. 2B). The interaction is replicated in the visual color change from colorless to yellow color.

To investigate the measurable response of synthesized probe **NG1** towards Cu^{2+}, the different concentration of **NG1**:Cu^{2+}complex was studied. The plot shows the linear relationship in the concentration range between 2.5 to 40 ppm. The limit of detection (LOD) is detected by UV−visible spectroscopy and is calculated by following formula

$$LOD = \frac{3\sigma}{Slope\ of\ calibration\ curve}$$

where the σ is the standard deviation.

LOD wascalculated to be 2.5 ppm from the plot of Absorbance vsCu^{2+}.concetration.

In conclusion, the conveniently visualized detection limit for the newly synthesized sensing probe **1** solution is 2.5 ppm for Cu^{2+} with naked eye without using any instrumentation, which is much lower according to the maximal permitted level of Cu^{2+}.The short response time and high selectivity for the probe 1 in visual inspection can be accounted for strong affinity.

The Job's plots were constructed to demonstrate complexation between Cu^{2+} and probe **1**. The indicative of 1:1complexation between Cu^{2+} and probe **1**. As the Job's plots reveal 1:1 binding stoichiometry between probe **1** and $Cu^{2+}$and suggest for bis-coordination of Cu^{2+} via nitrogen and Sulphur atom on the probe **1** (Scheme 2). Moreover, the interaction and binding behavior between probe **1** and Cu^{2+} is also evinced via FTIR and is presented in supporting information (Fig. S2). FTIR spectrum supports the change in characteristic peaks of probe **1** in aromatic region (1450-1650 cm^{-1}) due to interaction via nitrogen and sulphur atoms on the probe **1** with Cu^{2+}which prove the complex formation between probe **1**and Cu^{2+}. To further investigate the interaction between probe **1** and Cu^{2+}, the 1H NMR spectrum was also recorded. A significant upfield shift is assessed for imine group, which parts the overlapped signals between 8.0-8.5. The results can be accounted to the bis-coordination of Cu^{2+}via N, and S.

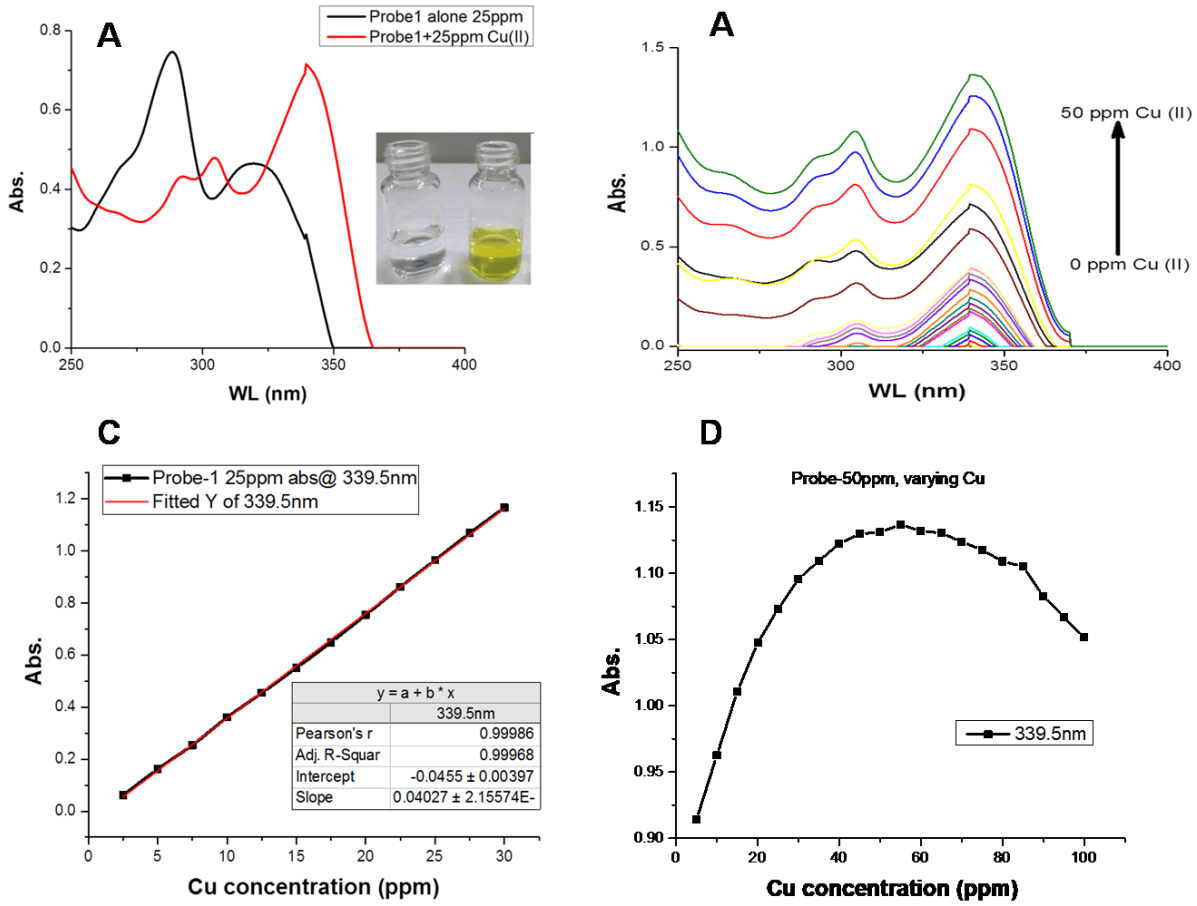

Figure 4. (A)UV-visible spectra of probe**NG1** with and without Cu^{2+}; (B) UV-visible spectra of probe NG**1** after sequential addition of Cu^{2+}; (C) LOD of detection of probe NG**1** by colorimetery; (D) Job's plot taking fixed concentration of probe NG**1** and varying concentrations of Cu^{2+} showing 1:1 stoichiometery. Vial images of NG**1** with Cu^{2+} and other metals showing yellow fluorescence and selectivity for Cu^{2+}

To assess the selectivity of probe NG**1**, the related experiments were performed in the presence of other ions for colorimetric response. As revealed in Fig. the color of probe**NG1** is least affected in the presence of other types of common ions (50 ppm: Na^{+}, Cu^{2+}, Fe^{3+}, Cd^{2+}, Mn^{2+}, Ag^{+}, Hg^{2+}, K^{+} , Mg^{2+}, Ca^{2+} and Cr^{3+}). Only Cu^{2+} presence results in the color change of probe NG**1**from colorless to yellow. The same results are evaluated with UV−visible spectroscopy and only Cu^{2+} containing vial exhibits a peak shift from 287 to 340 nm in comparison with other ions (taken separately) or in blank sample. Furthermore, even if all the ions except $Cu^{2+}$are added to

the probe NG**1**the solution, remain colorless, whereas the presence of Cu^{2+} leads to a typical transformation in the absorption band as detected by the UV−visible spectroscopy (ESI). The application of the assay was also tested for the detection of Cu^{2+}in real ground water samples. The results displayed an excellent selectivity for the copper detection as compared with the other ions. This indicates that the detection system has perfect selectivity for Cu^{2+} with negligible interference from other common ions during the analysis (ESI). The Cu^{2+}give the same colour intensity via binding with probe NG**1**. This is possible as the thiol and amine group can present in NG1 can interact withCu^{2+}. Thus, the present study realizes that the probe NG**1** can be used for the simultaneous detection of Cu^{2+} in real water samples as well as it could be potential used for sensing Cu^{2+} in mammalian cells and organisms.

Once the sensitivity and selectivity of probe NG**1** was ascertained by colorimetry, fluorescence assay was done in the presence of Cu^{2+}. Interestingly, it could be ascertained that NG**1** also reveals excellent fluorescence properties. When NG**1** was excited at 340 nm the emission spectra were obtained with the maxima at 440 nm. When Cu^{2+} was added in increasing concentration there was significant enhancement in the intensity and the graph exhibited red shift towards 470 nm. The sensitivity for the detection of Cu^{2+} was exceptionally good and as lowas 0.1 ppm.

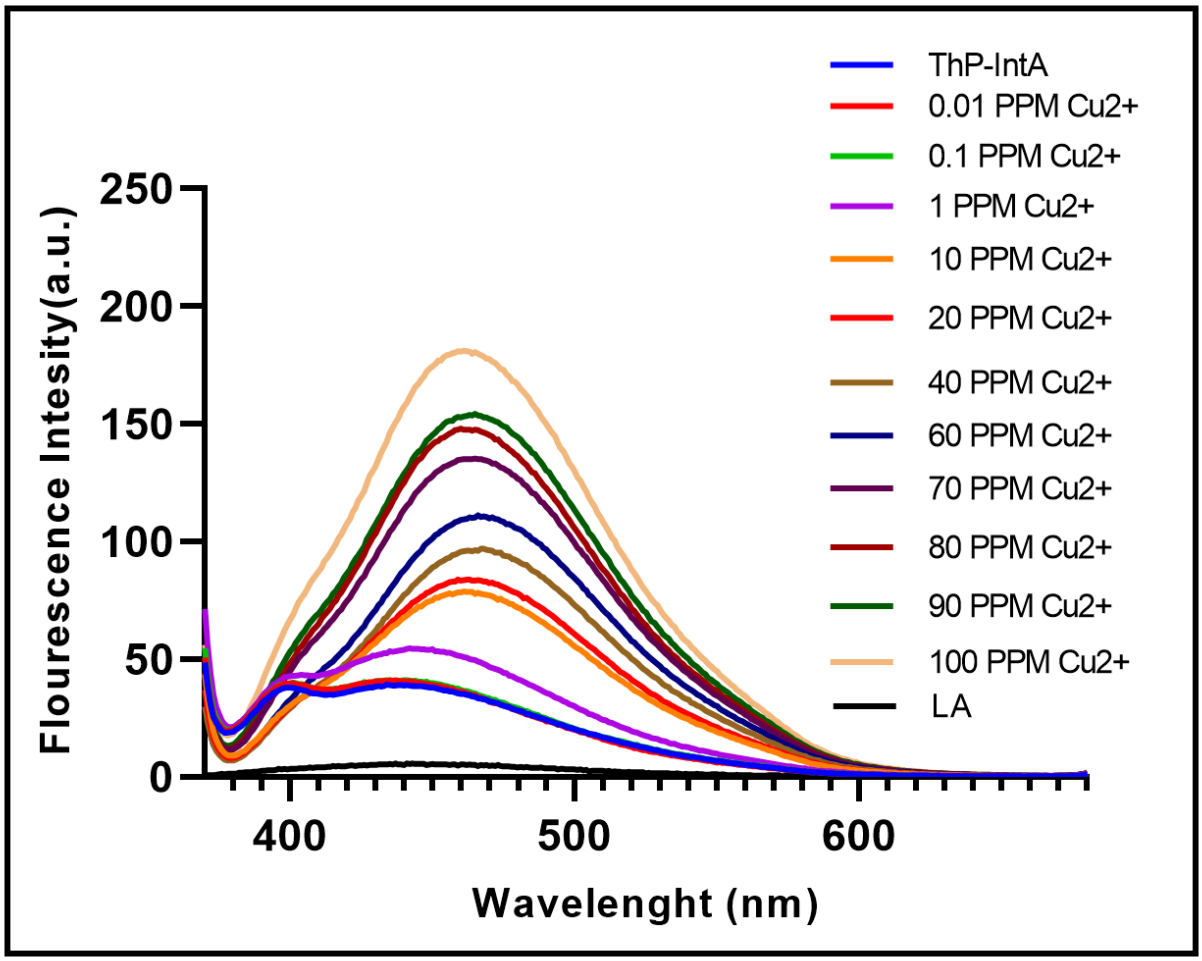

Figure 5. Fluorescence spectra of **1**(ThPInT A)in the presenceof varying concentration of Cu^{2+}(0.001 ppm -100 ppm) and quenching in presence of Lactic Acid (LA).

3.4.1 Molecular Geometries and Energetic Stabilities of Complexes

Fig.6shows the ground state optimized geometry of all three probes and their association with Cu as well as lactic acid. The binding energy (BE) of these complexes are elucidated as:

$$BE = E_{complex} - \Sigma E_{individual} (1)$$

Where, $E_{complex}$ contains the ground state energy of complex and $\Sigma E_{individual}$contains the sum of ground state of all molecule in a particular complex. The BE of all the optimized structures are presented in curly braces in Table 1.

Table 1. Optimized energy (in Hartree) and binding energy (in kcal/mol) of the Complex NG1, L2 and L3 with the Cu and Lactic Acid

	Optimized Energy (Hartree)	Position 1 with Cu (Hartree)	Position 2 with Cu (Hartree)	With Lactic Acid (Hartree)
NG1	-1254.4797	-2894.9918 {-25.06}	-2894.9658 {-8.71}	-3238.7456 {-112.10}
NG2	-1139.9170	-2780.4292 {-25.06}	-2780.4032 {-8.73}	-3124.1970 {-120.91}
NG3	-1123.8654	-2764.3567 {-11.97}	-2764.3385 {-0.55}	-3108.1511 {-124.46}

The binding energies in kcal/mol are provided in curly braces.

Initially the neat probes i.e. NG1, NG2 and NG3 was optimized using DFT calculations. Based on energetic stability, NG1 was found to the most stable ligand. To make a better comparison, along with NG1 other two probes (NG2 and NG3) were also interacted with Cu and lactic acid (see Fig.6). There were at least two different possibility of interaction of Cu with Ligand i) with the sulfur atom and ii) near the nitrogen atom. The BE calculations for the all complexes indicates that the complex 1 are the most stable complex. Here, Cu atom strongly interacts with the oxygen and sulfur atoms having bond length of 1.98 Å and 2.18 Å. In complex 2 (all the three probes), Cu atom is weakly coordinated with nitrogen and oxygen atoms as bond length increased on the interaction (Fig.6).

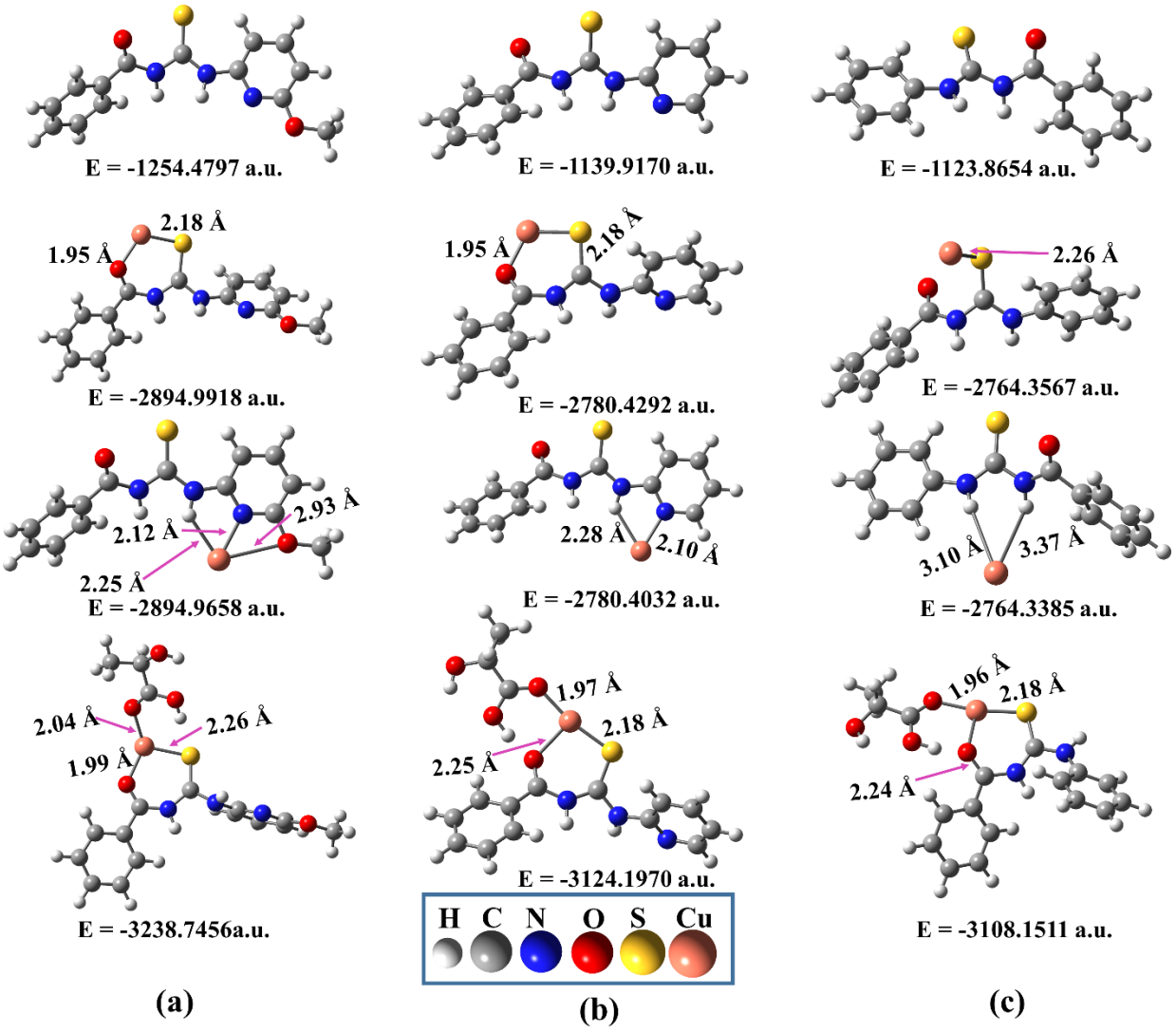

Figure 6:DFT computed optimized geometries of (a) NG1, NG1+Cu(1), NG1+Cu(2) and NG1+Cu+Lactic acid, (b) L2, L2+Cu(1), L2+Cu(2) and L2+Cu+Lactic acid, and (c) L3, L3+Cu(1), L3+Cu(2) and L3+Cu+Lactic acid with their optimized energy in Hartree.

As experimentally observed, on the interaction of Cu with NG1 yellow colored complex is obtained but when lactic acid is incorporated with this complex this yellow color quenches. To understand this behavior, we have introduced a molecule of lactic acid with this stable complex 1 of NG1 (Fig.6(a)). From Fig.6a (compare the structure of second and fourth geometry from the vertical position) it is noticeable that Cu is strongly binding with the sulfur and oxygen atom of NG1 through 2.18 Å and 1.95 Å respectively. However, upon complex with lactic acid both the bond strengths get weekend and calculated to be 2.26 Å and 1.99 Å respectively. It is the clear

indication of Cu binding with lactic acid and disturb the property of NG1+Cu complex. We have also optimized a dimer like structure of two NG1 with single Cu atom Fig.7(c) to check the assembly of Cu with more NG1 molecule and almost similar structure features are found as in single case.

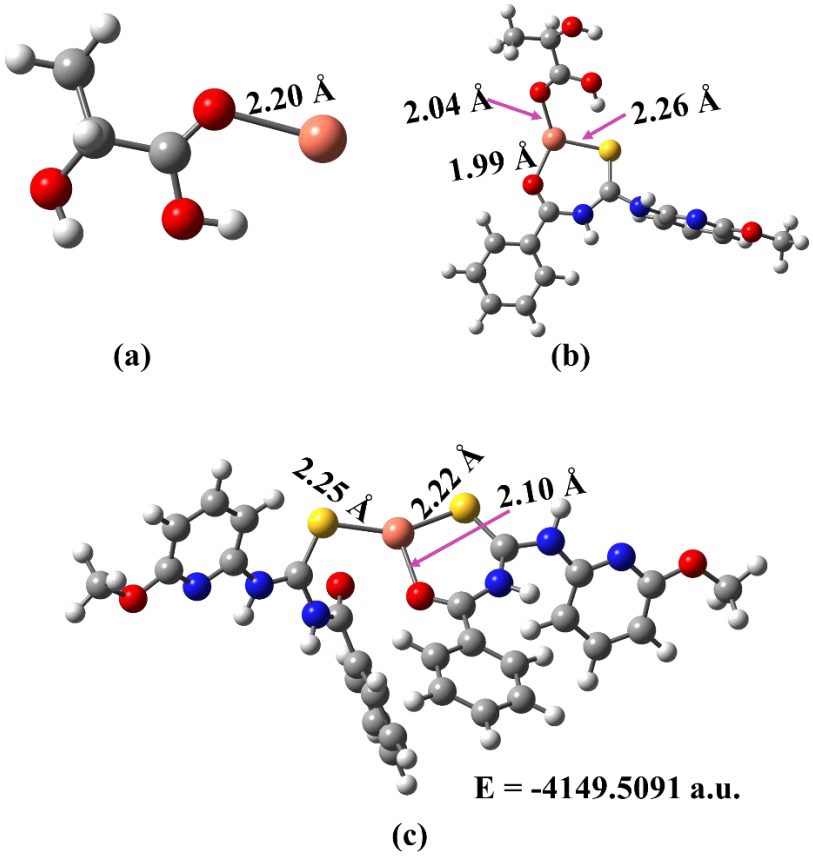

Figure 7. Optimized structures of (a) Lactic acid with Cu, (b) Probe NG1 with Cu and Lactic acid, and (c) self-associated dimer of NG1 bonded to single Cu-atom.

3.4.2 Electrostatic Potential (ESP) Mapped Electron Density Surfaces

Molecular electrostatic potential (MEP) (also called ESP) of a molecular association is correlated with the corresponding partial charges, dipole moment and chemical reactive sites. Mapping of any molecular system is the way to visualize the relative polarity of the studied molecules. The expression for the ESP at any point *r* in the space near the molecule is given by

$$V(r) = \sum \frac{z_A}{|R_A - r|} - \int \frac{\rho(r\prime)dr\prime}{|r' - r|} \quad (2)$$

Where, Z_A is the charge on the nucleus A studied at R_A and $\rho(r')$ the electron density. For probe NG1 and complex NG1with Cu and lactic acid, the electron density iso-surface on which the ESP surface was calculated and mapped is shown in Fig. 8. Recently, ESP mapping has played a remarkable role in geometrical arrangement, charge density analysis and polarity of different molecular system [25-28].

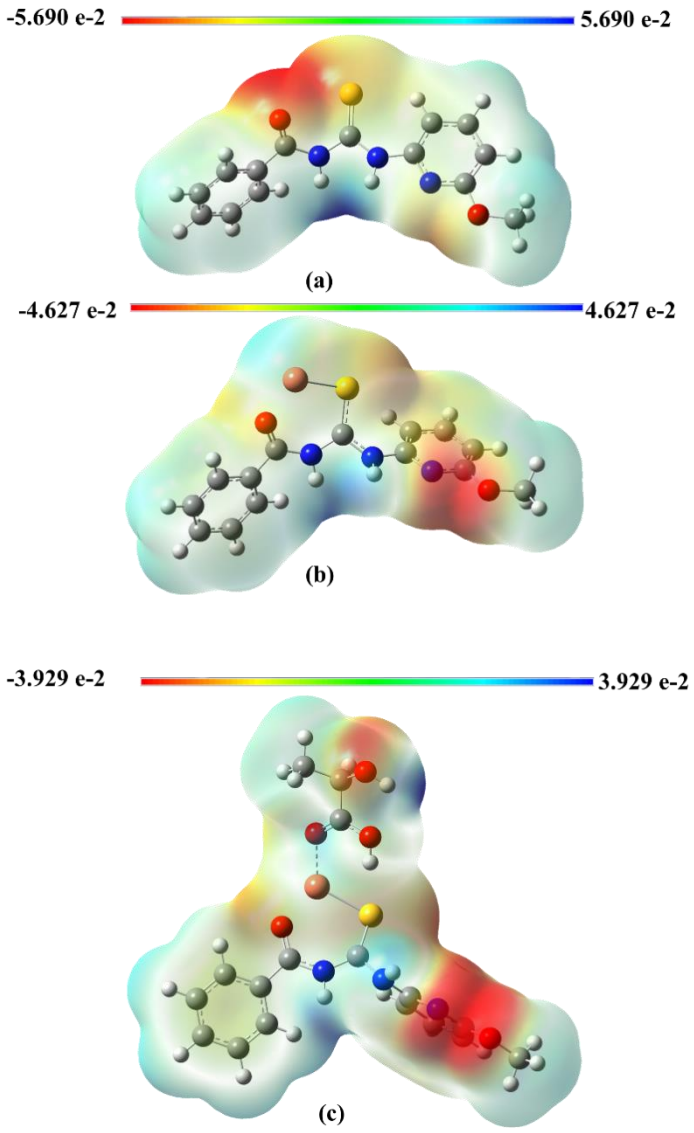

Figure 8. Electrostatic potential surfaces plotted from the total self consistent field (SCF) density having isovalue MO = 0.020000, density = 0.000400, calculated at the B3LYP level of theory. (a) Probe NG1, (b) Probe NG1 with Cu, and (c) Probe NG1 with Cu and Lactic acid .The red color indicates the most electronegativity, the blue color shows the most positive election density and the area of zero potential on the molecular surface represented by green colour.

As shown in the top panel of mapped optimized structure, the potential increases in the color code. The charge distribution over the neat probe NG1 with Cu and lactic acid is visualized in the ESP map in Figure 8. In neat NG1, nitrogen, oxygen and Sulphur are the three electronegative atoms, so it can be noticed a negative charge distribution over the both the oxygen as indicated by the red color whereas blue color over the benzene ring and both the nitrogen atom near Sulphur group indicates low electron density (Figure 8(a) as these atoms are less electronegative than oxygen). Shape and charge distribution are found to be considerably different in NG1 with Cu atom and lactic acid. Positive charge increases (blue color near the Cu atom) as Cu atom attaches with Sulphur in comparison with the neat NG1 and negative charge increases near the oxygen atom which is attached with $–CH_3$ group. Ongoing from NG1-Cu complex to NG1-Cu-lactic acid, positive charge increases around the Cu atom as Cu is binding with the oxygen atom of carboxylic group of lactic acid. The reason may be due to charge transfer from Cu to oxygen atom as it is known that Cu form copper lactate with lactic acid. This result clearly indicates that Cu is interacting more with lactic acid than the probe as yellow color of NG1+Cu quenches after interacting lactic acid which is experimentally observed.

3.4.3 Electronic absorption

TD-DFT calculated results were used to explain the experimentally measured absorption bands of the complexes probe**1**and probe **1**with Cu^{2+} in the presence of different ppm of Cu^{2+}. The frontier molecular orbitals of neat probe **1** and with Cu-atom, are shown in Fig. 9. Calculations show that the probe **1** reveals three bands at 427, 325 and 311 nm (experimentally observed at 290 nm in 30 % Water: Methanol). The theoretical calculated absorption at ~325 nm red-shifted when Cu^{2+} is added and absorption appears at ~680 nm, which shows the similar trend as of experimentally observed absorption bands. Energy bands calculated at ~325 and ~680 nm with oscillator strengths (f) 0.0844 and 0.1445 are due to electronic excitations from HOMO-1 — LUMO and HOMO—LUMO+1 and attributed to electron transfer from Sulphur atom to other part of probe NG**1**and from Sulphur to Cu^{2+} atom, respectively.For both complexes (neat probe

NG**1** and NG**1** with Cu-atom), the calculated bands are in good agreement with observed absorption bands and show similar trend.

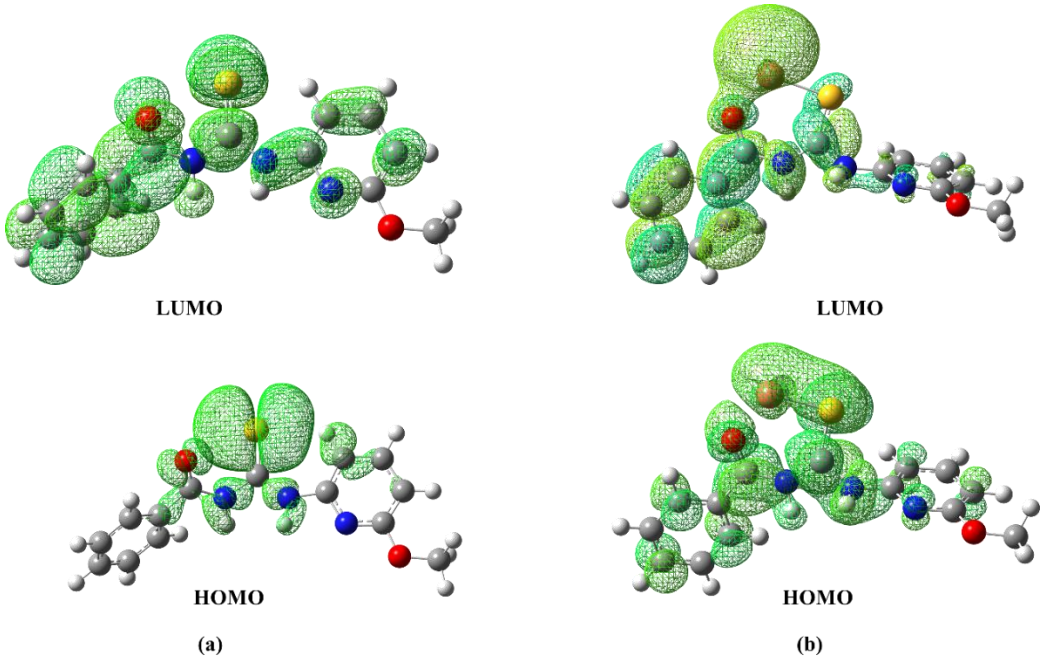

Figure 9. Molecular orbitals HOMO and LUMO of (a)neat **NG1** and (b)**NG1** with Cu^{2+}. The orbitals were obtained using an iso-surface value 0.02 e/$Å^3$.

Application of NG1-Cu complex in cell imaging and dual detection of Cu and lactate

The *invitro* sensing capabilities for NG1-Cu were further explored by testing its capacity to sense Cu^{2+} and lactate in mammalian cells. The application of **NG1-Cu**complex was tested in living cells by using **Cytotoxicity studies and cellular imaging.** Upon studying robust photo physical properties of these novel RGB emitting compounds, we decided to test for their biocompatibility and their *in cellulis* behavior.

Cell viability was measured by measuring absorbance of MTT at 570nm and calculated the ratio of absorbance of cells treated with respective compounds to that of control untreated cells. The results shown in Fig.2 indicate that PTC1 and Thp-IntA compounds have low cytotoxicity (~80% cell viability), strongly suggesting that these compounds can be further exploitedfor cellular imaging applications.To test for cell permeability and fluorescence property of NG1molecule in cells, experiments were carried out using retinal pigmented epithelial (RPE1) cells. The cells were pulsed with Thp-IntA in absence or presence of different concentrations of Cu^{2+} for 15 mins, fixed and imaged on confocal microscope. In accordance with *in vitro* data, imaging of fixed cells using confocal microscope displayed that these compounds are permeable in cells and show bright blue fluorescence in blue filter (shown in Fig.1).Interestingly, the fluorescence of the dye ThP IntA was highly enhanced in presence of exo-genous Cu^{2+}. This enhancement in cellular intensity of dye was rescued to background levels in presence of lactic acid, indicating the potential of dye to sense both Cu^{2+} and lactate from cells.

a. **MTT assay results -** MTT assays were carried out using a stock solution of 500:500 ppm ThP Int A:Cu. The stock was serially diluted and cells were grown in well containing 25, 50, 75, 100, 150, 200, 250 ThP:Cu complex in PPM. The best result were obtaine for 100ppm:50 ppm ThP:Cu and cell showed yellow fluorescence.

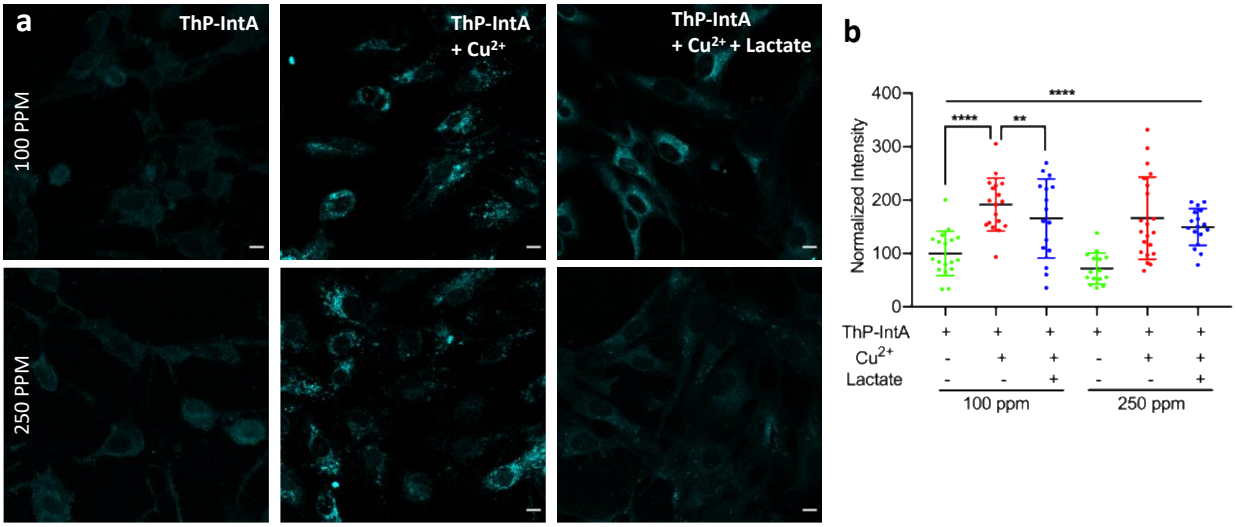

b. **Cellular imaging of Cu^{2+}in RPE1 cells withThP IntA-Cu complex.**Retinal epithelial pigmental cells (RPE1) were pulsed with 100 and 250 ppm of ThP IntA dye in absence or presence of Cu^{2+} in 1:1 ratio of dye:Cu^{2+}. Further the cells were incubated with lactate in presence of dye and Cu^{2+} for 15 min at 37ºC, fixed with paraformaldehyde and imaged on confocal microscope using 405 nm excitation laser and imaged acquired using broad width band-pass filters. The images were further quantified using imageJ for the cellular intensity of dye in various conditions and the normalized intensity plotted in right fig. Scale bar: 10 μm.

Experimental section

2.1 Materials

All the starting materials for **1** synthesis were obtained from commercial suppliers and used as received. 2-Amino-6-methoxypyridine and Benzoyl isothiocyanate were purchased from Combi-Blocks, USA. Acetone, THF, all metal ions were purchased from Sisco Research Laboratories (SRL), India. $Cu(NO_3)_2.2.5\ H_2O$ and $CuCl_2.\ 2H_2O$ was purchased from sigma. Lactic acid was purchased from Fluka.Moisture sensitive reactions were performed under an atmosphere of dry Nitrogen. All the solvents used for reactions were distilled prior to use. The water used for all the microscopy and spectroscopy measurement was ultra-pure obtained from Millipore Direct-Q® 5

UV Water Purification System. Column chromatography was carried out on silica gel (200–300 mesh). The $R_f$was recorded in Analytical TLC Silica Gel 60F254 purchased from Merck (Germany). The melting point of **1** and its derivatives was recorded in Visual Melting Range Apparatus (MR-VIS) provided by LABINDIA. ^{1}H NMR (400 MHz) and ^{13}C NMR (100 MHz) spectra were recorded on aAvance III 400 NMR spectrometer instrument. Proton chemical shifts were reported in parts per million. HPLC was done using Waters E2695 machine. HPLC was performed using ammonium bicarbonate buffer (ABC) 27 minutes run time and water: ACN as mobile phase in C-18 Column. LC-MS was obtained on Waters 2690 LC-MS instrument. The method used was Ammonium bicarbonate Buffer (ABC); 7 minutes run time and water: ACN as mobile phase in C-18 Column. UV-visible spectra were recorded on a LabIndia UV-Vis Spectrophotometer 3000+ with 10 mm quartz cell at 25 ^{0}C.

2.2 Synthesis of probe

In a three-necked round bottom flask, fitted with a dropping funnel 50ml of dry acetone was filled. 5.0g (27 mM) of 2-Amino 6-Methoxy pyridine was placed followed by drop wise addition of dry acetone under N_2 atmosphere during constant stirring of reaction mixture. Next, 7.2 g (44mM) of benzoyl isothiocyanate was added and the reaction mixture was then allowed to stir for another 2h at room temperature1. The progress of the reaction was monitored by analytical TLC by using the ethyl acetate-hexane (3:7) solvent mixture. After the completion of reaction, the reaction mixture was then poured carefully with stirring into 500 ml of cold water and the resulting yellow precipitate of (N-((6-methoxypyridin-2-yl)carbamothioyl)benzamide) is separated by suction filtration followed by washing of precipitate with water(3x100 ml). The filtrate was further purified by vacuum distillation which yielded desired product (10.0 g, 34mmol, Yields 86 %) as solid light yellow material.M.P.136 0C Rf 0.53, (This material was used in next step without any further purification. and probe 1 were also confirmed by EI- MS. The mass spectrum of**1** shows strong molecular peak at $M^+ + 1$=287.86. While the $M^+ + 1$ ion at appears for base peak. Similarly probe **2** and probe **3** was synthesized using amino pyridine and aniline respectively as substrate (Details of **2** and **3** synthesis is in ESI)

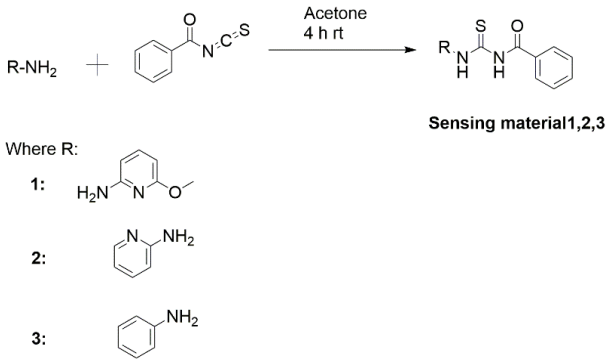

Scheme 1. |Schematicrepresentationof synthesis of the probes NG**1**, NG**2** and NG**3**

2.2 Self-assembling properties of NG1:

2.3 Colorimetric Detection of Copper

For colorimetric measurements,stock solutions of 500 ppm NG1 and 500 ppm$Cu(NO_3)_2.2.5\ H_2O$. were prepared. The sensitivity of probe NG1 for Cu^{2+} and other metal ions were tested by mixing 250 ppm probe **1** with 100 ppm metals (100 ppm: Cu^{2+}, Fe^{3+}, Cd^{2+}, Mn^{2+}, Ag^{+},Hg^{2+}, Ca^{2+}, Cr^{3+}, K^{+} , Mg^{2+} and Na^{+}). The LOD of probe NG1was detected by making a complex of 250 ppm:250 ppm **1**: Cu^{2+} complex. The stoichiometric ration of NG1: Cu complex was determined by adding varying concentrations of Cu^{2+} (0.5-50 ppm) to 50 ppm NG1.

2.4Fluorimetricassay for the detection of Cu^{2+} and lactic acid

For fluorometric measurements, 250 ppm of **1** stock was used and varying concentration of Cu^{2+} (.001-100 ppm) was added. For lactic acid mediated quenching 500 ppm of lactic acid was added to 250ppm:100 ppm **1**:Cu^{2+} complex.

2.5 Computational Details

The prediction of certain important molecular properties of the **ligand NG1, L2 and L3** and their possible complexes with Cu and lactic acid are calculated using density functional theory (DFT) calculations. All computational calculations were carried out using the *Gaussian 16* programming package in the presented works [15]. *GaussView 6* software was used to generate the input molecular structure and to analyze the output of all calculated results [16]. Geometric

optimization calculations were performed in the gas phase using DFT by employing the internally stored 6-311++G(d,p)[17,18,] and the hybrid density functional theory that incorporates B3LYP correlational functional [19,20] method. In general, B3LYP is a prominent method and preferable to the HF and MP2 method as it includes Becke's three-parameter exchange with Lee, Yang, and Parr's correlational functional as well as a HF exchange term. DFT calculations using the B3LYP protocol has been provided a meaningful and nice correlation with experimental results [21-24]. Time dependent density functional theory (TD-DFT) were also incorporated to compute electronic excitation energies and molecular frontier orbitals to analyze the charge transfer from Cu to probe. In addition, the mapping surfaces for 1 with electrostatic potential (ESP) was also shown to better understand the distribution of charges through shape, size and color code.

2.6**Cytotoxic assay:**To evaluate the biocompatibility of PTC1 and Thp-IntA compounds, we performed standard colorimetric MTT assay. Monkey kidney fibroblast cells were seeded at a density of 5 x 10^3 cells/well into 96-well plates and maintained in Dulbecco's modified Eagle's medium (DMEM) containing 10% fetal bovine serum (FBS) at 37ºC in a 5% CO_2incubator. After 24hrs once the cells are adhered to surface, the culture medium was replaced by fresh culture medium containing varying concentrations of PTC1 and Thp-IntA compounds and again incubated for 24hrs at 37ºC in a 5% CO_2incubator. After incubation, the medium was aspirated and replaced by 100µl/well of MTT prepared in DMEM medium to a final concentration of 0.5 mg/mL and the plate was incubated furtherfor 4 hrs at 37ºCin a 5% CO_2incubator. The formed formazan crystals were solubilized by adding 100µl of cell culture grade DMSO per well and incubated for 2hrs at 37ºCin a 5% CO_2incubator. The plate was gently shaken, and then the absorbance of purple formazan was recordedat 570 nm using a plate reader.

2.7 Cellularsensing of Cu2+: Retinal pigmental epithelial cells (RPE1) were Cells were seeded at a density of 1.5 x 10^5 cells/well in Dulbecco's modified Eagle's medium (DMEM) containing 10% fetal bovine serum (FBS) and incubated at 37ºC in a 5% CO_2 incubator for 24 h. The medium was replaced with 20mM HEPES buffer and incubated with dye ±Cu^{2+}± Lactic acid in the concentrations of 100 ppm and 250 ppm for 15 mins at 370C in water. Post incubation, the cells were washed with ice cold PBS++ to block endocytosis and removed the unbound dye and Cu2+. The cells were then fixed using 4% Paraformaldehyde for 10 mins at room temperature. The fixed coverslips were visualized for dye uptake using Leica SP8 confocal microscope. The cells were excited using 405 nm with very low laser power (~ 1% laser power) and the images were acquired using a

broad width emission spectrum to capture maximum of the emitted photons.50-60 cells were imaged in every condition using the same laser power and imaging conditions.

Data analysis: The image analysis and quantification were performed using ImageJ software (nih.gov). 50 cells were randomly selected to perform the quantification. Value of total fluorescence intensity of each cells were obtained from ImageJ. The images were quantified by substracting background and measuring the cellular intensities by measuring the areas of the cells and the total cellular intensity. Thenormalized mean value and standard deviationfor each was calculated and plotted in the graph using Prism 7 software and the statistical significance was calculated using one-way Anova test.

4. Conclusions

The sensitivity and specificity of **1** towards $Cu^{2+}$is tested by various spectroscopic and biophysical assay. Finally the supramolecular assembly of probe was studied and it suggests disaggregation mediated by Cu^{2+} may play a crucial role in producing yellow fluorescence.Further it was found that the yellow fluorescence is completely quenched on addition of Lactic acid suggesting the application of **1** for sequential detection of Cu and lactate. Since high levels of lactate and Cu are associated with many pathological disorders the results presented in the manuscript may be immense importance for designing a simple and cost-effective technique for dual detection of Cu^{2+} and lactate.

In addition to the experimental study, DFT calculations were also carried out various possible probes **1**, **2** and **3** with Cu atom and lactic acidto support our experimentally observed results. The comparison of experimental and theoretical results reveals a good agreement between experimental findings and calculated results and shows same pattern of shifting in absorption towards higher wavelength.

Funding sources

The work was supported by the DST SERB extramural research fund (Project No. EMR/2016/003186) received by Dr. NidhiGour and Dr. Manoj K. Pandey and DST-SERB Ramanujan Fellowship to Dhiraj Bhatia.

Author contributions

NG proposed the application of probe while VK synthesized the probe. The fluorescence studies were done by VK and ChamdraKanth jointly. SK and DB devised the cell culture experiments. SK performed the Cellular uptake and quantification of dye uptake in cells. All the authors discussed the results and contributed in manuscript drafting**.**

Acknowledgments

NG, MKP, BK and CKP greatly acknowledge support from DST and

SERB research grant (EMR/2016/003186) for funding and fellowships. DS thanks GSBTM for fellowship.We thank Central Imaging Facility (CIF) at IITGN for confocal microscopy and the initial seed funding from IITGN to Dhiraj Bhatia.

References

1. Valdez, C. E., Smith, Q. A., Nechay, M. R., &Alexandrova, A. N. (2014). Mysteries of metals in metalloenzymes. *Accounts of chemical research*, *47*(10), 3110-3117.
2. Mocchegiani, E., Costarelli, L., Giacconi, R., Piacenza, F., Basso, A., &Malavolta, M. (2012). Micronutrient (Zn, Cu, Fe)–gene interactions in ageing and inflammatory age-related diseases: implications for treatments. *Ageing research reviews*, *11*(2), 297-319.
3. Osredkar, J., &Sustar, N. (2011). Copper and zinc, biological role and significance of copper/zinc imbalance. *J Clinic Toxicol S*, *3*(2161), 0495.
4. Bremner, I. (1998). Manifestations of copper excess. *The American journal of clinical nutrition*, *67*(5), 1069S-1073S.
5. Fitzgerald, D. J. (1998). Safety guidelines for copper in water. *The American journal of clinical nutrition*, *67*(5), 1098S-1102S.
6. Bakkaus, E., Collins, R. N., Morel, J. L., &Gouget, B. (2006). Anion exchange liquid chromatography–inductively coupled plasma-mass spectrometry detection of the Co2+, Cu2+, Fe3+ and Ni2+ complexes of mugineic and deoxymugineic acid. *Journal of Chromatography A*, *1129*(2), 208-215.
7. Shamspur, T., Mostafavi, A., &Sheikhshoaie, I. (2008). Determination of copper in water and plant samples by flame atomic absorption spectrometry after preconcentration on octadecyl silica membrane disks modified with a recently synthesized Schiff's base. *Journal of Aoac International*, *91*(4), 865-870.
8. Ren, L. Chong, J., Loya, A., Kang2, Q., Stair, J. L., Nan, L., &Ren, G. (2015). Determination of Cu2+ ions release rate from antimicrobial copper bearing stainless steel by joint analysis using ICP-OES and XPS. *Materials Technology*, *30*(sup6), B86-B89.
9. Zhang, S., Niu, Q., Lan, L., & Li, T. (2017). Novel oligothiophene-phenylamine based Schiff base as a fluorescent chemosensor for the dual-channel detection of Hg2+ and Cu2+ with high sensitivity and selectivity. *Sensors and Actuators B: Chemical*, *240*, 793-800.

10. Kaur, P., Kaur, M., & Singh, K. (2011). Ferrocene based chemosensor for Cu2+—A dual channel signaling system. *Talanta*, *85*(2), 1050-1055.
11. Hamedan, N. A., Hasan, S., Zaki, H. M., & Alias, N. Z. (2017, February). Colorimetric chemosensor of symmetrical benzoylthiourea derivatives as for detection of Cu2+ in aqueous solution. In *IOP Conference Series: Materials Science and Engineering* (Vol. 172, No. 1, p. 012038). IOP Publishing.
12. Horak, E., Vianello, R., Hranjec, M., &Murković Steinberg, I. (2018). Colourimetric and fluorimetric metal ion chemosensor based on a benzimidazolefunctionalised Schiff base. *Supramolecular Chemistry*, *30*(10), 891-900.
13. Khairul, W. M., Zuki, H. M., Hasan, M. F. A., &Daud, A. I. (2016). Pyridine Acyl Thiourea as Ionophore for the Detection of Copper (II) in Aqueous Phase. *Procedia Chemistry*, *20*, 105-114.
14. Jung, H. S., Kwon, P. S., Lee, J. W., Kim, J. I., Hong, C. S., Kim, J. W., ... & Kim, J. S. (2009). Coumarin-derived Cu2+-selective fluorescence sensor: synthesis, mechanisms, and applications in living cells. *Journal of the American Chemical Society*, *131*(5), 2008-2012.
15. Frisch, M. J.; Trucks, G. W.; Schlegel, H. B.; Scuseria, G. E.; Robb, M. A.; Cheeseman, J. R.; Scalmani, G.; Barone, V.; Petersson, G. A.; Nakatsuji, H.; Li, X.; Caricato, M.; Marenich, A. V.; Bloino, J.; Janesko, B. G.; Gomperts, R.; Mennucci, B.; Hratchian, H. P.; Ortiz, J. V.; Izmaylov, A. F.; Sonnenberg, J. L.; Williams-Young, D.; Ding, F.; Lipparini, F.; Egidi, F.; Goings, J.; Peng, B.; Petrone, A.; Henderson, T.; Ranasinghe, D.; Zakrzewski, V. G.; Gao, J.; Rega, N.; Zheng, G.; Liang, W.; Hada, M.; Ehara, M.; Toyota, K.; Fukuda, R.; Hasegawa, J.; Ishida, M.; Nakajima, T.; Honda, Y.; Kitao, O.; Nakai, H.; Vreven, T.; Throssell, K.; Montgomery, J. A., Jr.; Peralta, J. E.; Ogliaro, F.; Bearpark, M. J.; Heyd, J. J.; Brothers, E. N.; Kudin, K. N.; Staroverov, V. N.; Keith, T. A.; Kobayashi, R.; Normand, J.; Raghavachari, K.; Rendell, A. P.; Burant, J. C.; Iyengar, S. S.; Tomasi, J.; Cossi, M.; Millam, J. M.; Klene, M.; Adamo, C.; Cammi, R.; Ochterski, J. W.; Martin, R. L.; Morokuma, K.; Farkas, O.; Foresman, J. B.; Fox, D. J. Gaussian 16, Revision B.01; Gaussian, Inc.; Wallingford CT, 2016.
16. Dennington, R.; Keith, T. A.; Millam, J. M.GaussView, version 6; Semichem Inc.: Shawnee Mission, KS, 2016.
17. McAllister, M. A. Characterization of low-barrier hydrogen bonds 2. HF_2^-: a density functional and ab initio study. **1998**, *427*, 39-53.
18. Singh, D. K.; Cha, S.; Nam, D.; Cheong, H.; Joo, S.-W.; Kim, D. Raman Spectroscopic Study on Alkyl Chain Conformation in 1-Butyl-3-methylimidazolium Ionic Liquids and their Aqueous Mixtures. *ChemPhysChem***2016**, *17*, 3040-3046.
19. Becke, A. Density-Functional Exchange-Energy Approximation with Correct Asymptotic Behavior. *Phys Rev A* **1988**, *38* (6), 3098–3100.
20. Becke, A. D. Density-functional Thermochemistry. III. The Role of Exact Exchange. *J Chem. Phys.* **1993**, *98* (7), 5648–5652.
21. Singh, S.; Srivastava, S. K.; Singh, D. K. Hydrogen Bonding Patterns in Different Acrylamide–Water Clusters: Microsolvation Probed by Micro Raman Spectroscopy and DFT Calculations. *RSCAdvances* **2014**, *4*, 1761-1774.

22. Singh, D.; Asthana, B.; vastava, S. Modeling the Weak Hydrogen Bonding of Pyrrole and Dichloromethane through Raman and DFT Study. *J Mol Model* **2012**, *18* (8), 3541–3552.
23. Singh, D.; Vikram, K.; Singh, D. K.; Kiefer, W.; Singh, R. K. Raman and DFT Study of Hydrogen-bonded 2- and 3-chloropyridine with Methanol. *J Raman Spectrosc* **2008**, *39* (10), 1423–1432.
24. Singh, D. K.; Srivastava, S. K.; Schlücker, S.; Singh, R. K.; Asthana, B. Self-association and Hydrogen Bonding of Propionaldehyde in Binary Mixtures with Water and Methanol Investigated by Concentration-dependent Polarized Raman Study and DFT Calculations. *J. Raman Spectros.* **2011**, *42* (4), 851–858.
25. Bharti, A.; Bharati, P.; Dulare, R.; Bharty, M. K.; Singh, D. K.; Singh, N. K. Studies on Phenylmercury(II) Complexes of Nitrogen–Sulfur Ligands: Synthesis, Spectral,Structural Characterization, TD-DFT and Photoluminescent Properties. *Polyhedron* **2013**, *65*, 170–180.
26. Khandelwal, P.; Singh, D. K.; Sadhu, S.; Poddar, P. Study of the Nucleation and Growth of Antibiotic Labeled Au NPs and Blue Luminescent Au 8 Quantum Clusters for Hg 2+ Ion Sensing, Cellular Imaging and Antibacterial Applications. *Nanoscale* **2015**, *7* (47), 19985–20002.
27. Majumdar, D.; Dey, S.; Das, D.; Singh, D. K.; Das, S.; Bankura, K.; Mishra, D. Heterometallic Zn (II)-K (I) complex with salen-type Schiff-base ligand: Synthesis, crystal structure, solid-state photoluminescent property and theoretical study. *J. Mol.Structure.***2019**, *1185*, 112-120.
28. Sanchora,P.; Pandey,D. K.;Rana,D.;Materny,A.; Singh,D. K.Impact of Size and Electronegativity of Halide Anions on Hydrogen Bonds and Properties of 1-Ethyl-3-Methylimidazolium-Based Ionic Liquids. *J. Phys. Chem. A*DOI:10.1021/acs.jpca.9b04116
29.